# Syntheses, Crystal Structures and Different Magnetic Behaviors of Three Cyanide-bridged $Fe^{II}$-$M^{II}$ (M = Fe, Co and Mn) Complexes①

HUANG Ying-Ying[a, b, c] XU Qing-Dou[b, c] HU Sheng-Min[b]
WU Xin-Tao[b] SHENG Tian-Lu[b②]

[a] (*College of Chemistry, Fuzhou University, Fuzhou* 350002, *China*)

[b] (*State Key Laboratory of Structural Chemistry, Fujian Institute of Research on the Structure of Matter, Chinese Academy of Sciences, Fuzhou* 350002, *China*)

[c] (*University of Chinese Academy of Sciences, Beijing* 100049, *China*)

**ABSTRACT** Three dinuclear cyanide-bridged complexes $[Fe^{II}(PY_5OMe_2)CNM^{II}(PY_5OMe_2)](OTf)_3$ (M = Fe **1**, M = Co **2**, M = Mn **3**) ($PY_5OMe_2$ = 2,6-bis-((2-pyridyl)methoxymethane)pyridine OTf = $CF_3SO_3^-$) have been synthesized and characterized. Single-crystal diffraction analyses show these three dinuclear compounds are very similar in structure. The measured *ν*(CN) results for compounds **1**~**3** suggest that $Mn^{2+}$ is electron-poorer than $Fe^{2+}$ and $Co^{2+}$. Meanwhile, the temperature dependence of magnetic susceptibilities of complexes **1**~**3** reveals that in these three complexes, all the cyanide-carbon coordinated Fe(II) is low-spin, and Co(II) for **2** and Mn(II) for **3** are both in a high-spin state through 2~400 K but the cyanide-nitrogen coordinated Fe(II) for complex **1** exhibits spin crossover (SCO) behavior over 300 K and a hysteresis of 36 K in both cooling and heating modes.

**Keywords: cyanide-bridged, magnetic property, spin crossover; DOI: 10.14102/j.cnki.0254–5861.2011–3123**

## 1 INTRODUCTION

In the past decades, cyanide-bridged compounds have attracted the attention of many researchers because of their interesting magnetic coupling between paramagnetic metal centers[1, 2] and metal-to-metal charge transfer properties[3-5]. So far, a large number of cyanide-bridged compounds with novel structures and fascinating magnetic properties such as single-chain magnets (SCM)[6-10], single-molecule magnets (SMM)[11-16] and spin crossover (SCO)[17-22] have been reported. Among them, SCO complexes can switch between low spin (LS) and high spin (HS) states under the stimulation of external conditions such as light[17], pressure[23] and temperature[21] which are usually accompanied by the change of material physical properties like magnetic, optics and dielectric properties. Therefore, spin crossover complex is one of the most attractive advanced switchable materials with the potential to be used as molecular switches, data storage and data displays[24, 25]. Although this area has been studied for a long time, most of them focused on the effect of ligand field on metal ion spin state. There are few studies on the spin-crossover behavior of different metal ions in the same ligand filed.

In view of many SCO behaviors which are more common on octahedral transition metal complexes of $d^4$-$d^7$ electronic configuration coordinated by six nitrogen-based ligands[26, 27], we decide to use 2,6-bis-((2-pyridyl)methoxymethane)pyridine ($PY_5OMe_2$) ligand and cyanide-bridge as N-donor ligands to synthesize octahedral coordination compounds and investigate their spin transition behaviors. Herein, we report three dinuclear cyanide-bridged compounds which have been synthesized and characterized by IR spectroscopy, single-crystal X-ray diffraction analysis and magnetic properties analysis. For better comparison, three adjacent transition metal ions Mn(II), Fe(II) and Co(II) are used as the central metal ions to coordinate with 2,6-bis-((2-pyridyl)methoxymethane)pyridine ($PY_5OMe_2$) ligand to form the $[M^{II}(PY_5OMe_2)]^{2+}$ (M = Fe, Co and Mn) fragment and

Received 27 January 2021; accepted 4 March 2021 (**CCDC 2055113, 2055114 and 2055115**)

① This research was supported by the National Natural Science Foundation of China (21773243, 21973095) and the Strategic Priority Research Program of the Chinese Academy of Sciences (XDB20010200)

② Corresponding author. Sheng Tian-Lu, E-mail: tsheng@fjirsm.ac.cn

further combine with mononuclear complex $[Fe^{II}(PY_5O\ Me_2)\text{-}CN]^+$ through cyanide-bridge. The obtained three dinuclear complexes $[Fe^{II}(PY_5OMe_2)CNM^{II}(PY_5OMe_2)](OTf)_3$ (M = Fe **1**, Co **2** and Mn **3**) possess similar structures but obviously different magnetic behaviors.

## 2 EXPERIMENTAL

### 2. 1 Materials and physical measurements

Unless otherwise description, the experiments are under argon atmosphere and operated with the standard Schlenk techniques. Except that tetrahydrofuran is an ultra-dry solvent (water ⩽ 30 ppm), other chemical solvents are purchased at reagent grade without further purification. $[M^{II}(PY_5OMe_2)](OTf)_2$ (M = Fe, Co and Mn) were synthesized through the published papers[28, 29]. Infrared (IR) spectra in the range of 4000~400 $cm^{-1}$ were performed on a VERTEX 70 spectrophotometer with KBr pellet. The elemental analyses (C, H and N) were recorded on a Vario MICRO elemental analyzer. Variable-temperature magnetic susceptibility and field dependence of the magnetization measurements were conducted on a Quantum Design Magnetic Property Measurement System MPMS-XL magnetometer. Pascal's constants were used to correct the diamagnetism of complexes **1**~**3**[30]. And the thermal analyses were performed on a STA449C comprehensive thermal analyzer from 300 to 850 K at a heating rate of 20 K·$min^{-1}$ under nitrogen flow.

### 2. 2 Synthesis of the complexes

Since complexes **1**~**3** were prepared in a similar way, only the preparation of complex **1** is described in detail here.

#### 2. 2. 1 $[Fe^{II}(PY_5OMe_2)CN](OTf)$

KCN (1.95 g, 30 mmol) and $[Fe^{II}(PY_5OMe_2)](OTf)_2$ (2.49 g, 3 mmol) were added in methanol (30 mL ). The mixture was refluxed at 80 ℃ for about 0.5 hours. Then the solvent was removed in a vacuum and the remaining solids were extracted with $CH_2Cl_2$. The dark red product was obtained by removing $CH_2Cl_2$ solvent under reduced pressure and recrystallized in methanol. Yield: 1.71 g, 81%. Anal. Calcd. (%) for $C_{31}H_{25}F_3FeN_6O_5S{\cdot}CH_3OH$: C, 52.04; H, 3.96; N, 11.38. Found (%): C, 52.02; H, 3.98; N, 11.33.

#### 2. 2. 2 $[Fe^{II}(PY_5OMe_2)CNFe^{II}(PY_5OMe_2)](OTf)_3{\cdot}2H_2O{\cdot}3CH_3CN$ (**1**)

$[Fe^{II}(PY_5OMe_2)CN](OTf)$ (0.0706 g, 1 mmol) and $[Fe^{II}(PY_5OMe_2)](OTf)_2$ (0.0829 g, 1 mmol) were added in methanol (15 mL). The reaction mixture was refluxed with stirring at 80 ℃ for about 6 hours, after which the mixture solution was concentrated under reduced pressure, and then the product is precipitated by the addition of diethyl ether. The obtained product was redissolved in acetonitrile (8 mL), obtaining brown red crystals by slow diffusion of diethyl ether into the acetonitrile solution. Yield: 0.115 g, 75%. Anal. Calcd. (%) for $C_{62}H_{50}F_9Fe_2N_{11}O_{13}S_3{\cdot}2H_2O$: C, 47.37; H, 3.46; N, 9.80. Found (%): C, 47.27; H, 3.41; N, 9.78.

#### 2. 2. 3 $[Fe^{II}(PY_5OMe_2)CNCo^{II}(PY_5OMe_2)](OTf)_3{\cdot}2H_2O{\cdot}3CH_3CN$ (**2**)

The synthesis procedure was the same as complex **1** with $[Fe^{II}(PY_5OMe_2)CN](OTf)$ (0.0706 g, 1 mmol) and $Co^{II}(PY_5OMe_2)[OTf]_2$ (0.0832 g, 1 mmol) in 15 mL methanol. The orange red crystals were obtained. Yield: 0.121 g, 78%. Anal. Calcd. (%) for $C_{62}H_{50}CoF_9FeN_{11}O_{13}S_3{\cdot}2H_2O$: C, 47.28; H, 3.46; N, 9.78. Found (%): C, 47.37; H, 3.38; N, 9.87.

#### 2. 2. 4 $[Fe^{II}(PY_5OMe_2)CNMn^{II}(PY_5OMe_2)](OTf)_3$ (**3**)

The synthesis procedure was the same as complex **1**: $[Fe^{II}(PY_5OMe_2)CN](OTf)$ (0.0706 g, 1 mmol) and $Mn^{II}(PY_5OMe_2)[OTf]_2$ (0.0828 g, 1 mmol) in 15 mL methanol. The dark red crystals were obtained. Yield: 0.109 g, 71%. Anal. Calcd. (%) for $C_{62}H_{50}F_9FeMnN_{11}O_{13}S_3$: C, 48.51; H, 3.28; N, 10.04. Found (%): C, 48.58; H, 3.77; N, 9.47.

### 2. 3 X-ray structure determination

The crystallographic data of complex **2** were collected using an $\omega$-scan model technique on a Saturn724+ CCD diffractometer with graphite-monochromatic Mo$K\alpha$ ($\lambda$ = 0.71073 Å). Complexes **1** and **3** were on a MetalJet D2+ diffractometer with graphite-monochromatic Ga$K\alpha$ ($\lambda$ = 1.3405 Å). These structures were solved by direct methods using Fourier difference techniques with the SHELXL-2018/3 program package[31] and refined by full-matrix least-squares method on $F^2$ with anisotropic thermal parameters for the non-hydrogen atoms. All the hydrogen atoms were calculated and generated in the ideal positions.

## 3 RESULTS AND DISCUSSION

### 3. 1 X-ray crystal structure

Complexes **1**~**3** were synthesized by solution method and their crystals were obtained by slow diffusion of diethyl ether into the acetonitrile solution. Single-crystal X-ray diffraction analyses show that in the cation of compounds **1**~**3** the two cation fragments $[Fe(PY_5OMe_2)]^{2+}$ and $[M(PY_5OMe_2)]^{2+}$ (M = Fe, Co or Mn) with similar coordination structures are linked via a single cyanide bridge.

Compounds **1**, **2** and **3** crystallize in the monoclinic space group $P2_1/c$, $P2_1/c$ and triclinic space group $P\bar{1}$, respectively (Table 1 and Fig. 1). However, the structure of compound **3** contains two crystallographically independent molecules per asymmetric unit (Table 1 and Fig. S1). The central metal ions of the $[M(PY_5OMe_2)]^{2+}$ fragment possess the hexa-coordination environment with six nitrogen atoms from one $PY_5OMe_2$ ligand and one cyanide bridging ligand, forming a distorted octahedral geometry. But for compound **3**, the atoms of Fe−C≡N and C≡N−Mn in the backbone structure are disordered in position, as shown in Fig. S1. Thus, herein the structural parameters of compound **3** are not described for comparison.

**Table 1. Crystallographic Data for Complexes 1~3**

| | **1** | **2** | **3** |
|---|---|---|---|
| Chemical formula | $C_{62}H_{50}F_9Fe_2N_{11}O_{13}S_3{\cdot}2H_2O{\cdot}3CH_3CN$ | $C_{62}H_{50}CoF_9FeN_{11}O_{13}S_3{\cdot}2H_2O{\cdot}3CH_3CN$ | $C_{62}H_{50}F_9FeMnN_{11}O_{13}S_3$ |
| Formula weight | 1695.20 | 1698.28 | 1535.10 |
| *T* (K) | 100(2) | 100(2) | 200(2) |
| Color and habit | Red prism | Red prism | Red prism |
| Crystal size (mm) | 0.31 × 0.21 × 0.18 | 0.51 × 0.28 × 0.19 | 0.35 × 0.15 × 0.12 |
| Crystal system | Monoclinic | Monoclinic | Triclinic |
| Space group | $P2_1/c$ | $P2_1/c$ | $P\bar{1}$ |
| *a* (Å) | 12.41240(10) | 12.3934(3) | 12.9145(4) |
| *b* (Å) | 35.1871(3) | 35.4776(6) | 12.9482(3) |
| *c* (Å) | 16.25860(10) | 16.3918(3) | 20.6481(4) |
| *α* (°) | 90 | 90 | 89.6328(16) |
| *β* (°) | 97.0630(10) | 96.895(2) | 84.5167(19) |
| *γ* (°) | 90 | 90 | 84.809(2) |
| *V* (Å$^3$) | 7047.16(9) | 7155.2(3) | 3422.85(14) |
| *Z* | 4 | 4 | 2 |
| $\rho_{calc}$ (g/cm$^3$) | 1.598 | 1.577 | 1.489 |
| $\mu$ (mm$^{-1}$) | 3.329 (Ga*Kα*) | 0.623 (Mo*Kα*) | 3.045 (Ga*Kα*) |
| *F*(000) | 3480 | 3484 | 1564 |
| *θ* (°) | 4.37～104.09 | 3.40～52.74 | 5.96～104.09 |
| *GOF* | 1.066 | 1.067 | 1.051 |
| $R_{int}$ | 0.0655 | 0.0581 | 0.1014 |
| *R*, *wR* ($I > 2\sigma(I)$) | 0.0565, 0.1423 | 0.0487, 0.1260 | 0.0777, 0.1887 |
| *R*, *wR* (all data) | 0.0596, 0.1444 | 0.0561, 0.1313 | 0.0893, 0.1963 |

$R = \Sigma(||F_o| - |F_c||)/\Sigma|F_o|$;
$wR = [\Sigma w(|F_o^2| - |F_c^2|)^2/\Sigma w|F_o^2|^2]^{1/2}$

As shown in Table 2, the bond angles of C≡N–M (M = Fe and Co) and Fe–C≡N in **1** and **2** are nearly linear in ranges of 176.6(2)~177.1(3)° and 177.8(2)~178.0(3)°. The average Fe–N distances of $[Fe(PY_5OMe_2)CN]^+$ are 1.985(3) Å in **1** and 2.021(2) Å in **2**, which are in good agreement of the bond lengths for LS Fe(II) complexes[32], suggesting the cyanide-carbon coordinated Fe(II) is of low-spin. And the average M–N (M = Fe, Co) distances of cyanide-nitrogen coordinated metal ions are 1.997(3) Å in **1** and 2.080(2) Å in **2**. These are typical bond lengths for a LS Fe(II) complex and a HS Co(II) complex[34-37], which are consistent with the following magnetic data. We have tried to figure out the changes in bond lengths of **1** at high temperature, at which, however, the crystal was prone to collapse, thus precluding us from obtaining its crystallographic data at 400 K.

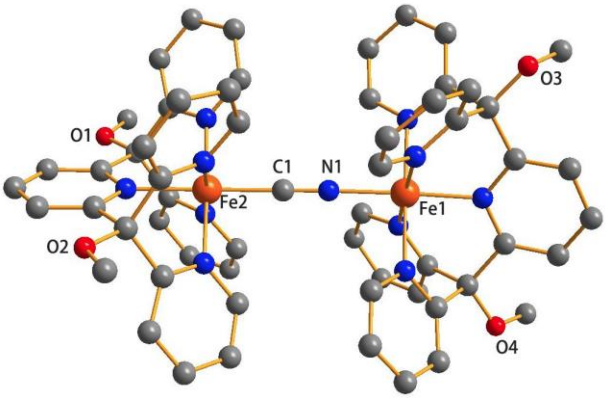


**Fig. 1a. Structure of complex 1 (All the H atoms, $CF_3SO_3^-$ anions and solvent molecules have been removed)**

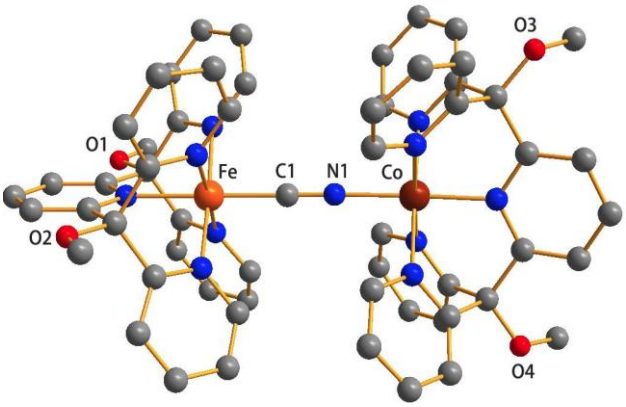


**Fig. 1b. Structure of complex 2 (All the H atoms, $CF_3SO_3^-$ anions and solvent molecules have been removed)**

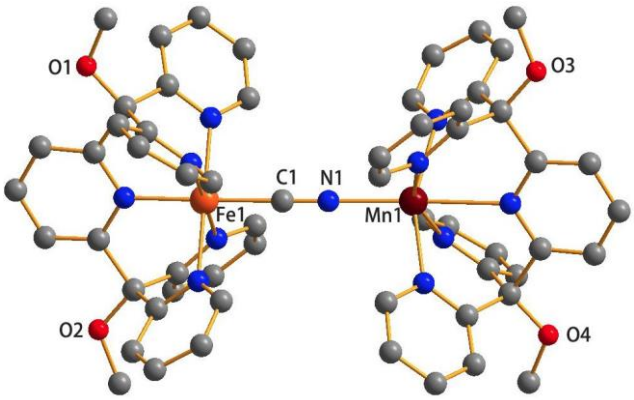


**Fig. 1c. Structure of complex 3 (The positional disordered atoms, all the H atoms, $F_3SO_3^-$ anions and solvent molecules have been removed for clarity)**

**Table 2. Selected Bond Lengths (Å) and Bond Angles (°) for Complexes 1～3**

| Compound **1** | | Compound **2** | | Compound **3**(**a**) | | Compound **3**(**b**) | |
|---|---|---|---|---|---|---|---|
| Fe(1)–N(1) | 1.925(3) | Co–N(1) | 1.994(2) | Mn(1)–N(1) | 2.132(6) | Mn(2)–N(7) | 2.113(5) |
| Fe(1)–N(2) | 2.040(3) | Co–N(2) | 2.124(2) | Mn(1)–N(2) | 2.182(6) | Mn(2)–N(8) | 2.174(7) |
| Fe(1)–N(3) | 1.962(3) | Co–N(3) | 2.040(2) | Mn(1)–N(3) | 2.119(6) | Mn(2)–N(9) | 2.127(7) |
| Fe(1)–N(4) | 2.005(3) | Co–N(4) | 2.088(2) | Mn(1)–N(4) | 2.466(4) | Mn(2)–N(10) | 2.423(4) |
| Fe(1)–N(5) | 1.990(3) | Co–N(5) | 2.074(2) | Mn(1)–N(5) | 2.094(6) | Mn(2)–N(11) | 2.142(7) |
| Fe(1)–N(6) | 2.062(3) | Co–N(6) | 2.158(2) | Mn(1)–N(6) | 2.171(6) | Mn(2)–N(12) | 2.129(7) |
| Fe(1)–N(7) | 1.998(3) | Fe–N(7) | 2.018(2) | Fe(1)–N(2) | 2.053(6) | Fe(2)–N(8) | 2.112(7) |

To be continued

| | | | | | | | |
|---|---|---|---|---|---|---|---|
| Fe(2)–N(8) | 1.996(3) | Fe–N(8) | 2.013(2) | Fe(1)–N(3) | 2.091(6) | Fe(2)–N(9) | 2.097(7) |
| Fe(2)–N(9) | 2.032(3) | Fe–N(9) | 2.055(2) | Fe(1)–N(4) | 2.000(4) | Fe(2)–N(10) | 2.005(5) |
| Fe(2)–N(10) | 1.991(3) | Fe–N(10) | 2.008(2) | Fe(1)–N(5) | 2.120(6) | Fe(2)–N(11) | 2.093(7) |
| Fe(2)–N(11) | 1.997(3) | Fe–N(11) | 2.013(2) | Fe(1)–N(6) | 2.108(6) | Fe(2)–N(12) | 2.106(7) |
| Fe(2)–C(1) | 1.910(3) | Fe–C(1) | 1.904(3) | Fe(1)–C(1) | 1.948(6) | Fe(2)–C(31) | 1.957(5) |
| N(1)≡C(1) | 1.164(5) | N(1)≡C(1) | 1.145(3) | N(1)≡C(1) | 1.153(8) | N(7)≡C(31) | 1.150(10) |
| C(1)≡N(1)–Fe(1) | 177.1(3) | C(1)≡N(1)–Co | 176.6(2) | C(1)≡N(1)–Mn(1) | 179.1(15) | C(31)≡N(7)–Mn(2) | 178.4(9) |
| N(1)–Fe(1)–N(2) | 89.63(11) | N(1)–Co–N(2) | 90.89(8) | N(1)–Mn(1)–N(2) | 102.3(5) | N(8)–Mn(2)–N(9) | 80.9(2) |
| N(1)–Fe(1)–N(3) | 177.76(2) | N(1)–Co–N(3) | 177.97(8) | N(1)–Mn(1)–N(4) | 174.6(6) | N(9)–Mn(2)–N(11) | 157.8(2) |
| N(1)≡C(1)–Fe(2) | 178.0(3) | N(1)≡C(1)–Fe | 177.8(2) | N(1)≡C(1)–Fe(1) | 178.3(11) | N(7)≡C(31)–Fe(2) | 178.5(10) |
| C(1)–Fe(2)–N(7) | 92.31(11) | C(1)–Fe–N(7) | 92.68(9) | C(1)–Fe(1)–N(2) | 89.5(4) | C(31)–Fe(2)–N(8) | 89.3(5) |
| C(1)–Fe(2)–N(9) | 178.86(3) | C(1)–Fe–N(9) | 178.98(9) | C(1)–Fe(1)–N(4) | 77.6(4) | C(31)–Fe(2)–N(10) | 179.1(6) |

### 3. 2 IR spectroscopy

IR spectra of complexes **1**~**3** are listed in Table 3, and the data of the parent mononuclear compound $[Fe^{II}(PY_5OMe_2)CN](OTf)$ are also listed for the purpose of comparison. Compared with $[Fe^{II}(PY_5OMe_2)CN](OTf)$ ($\nu_{CN}$ = 2087 $cm^{-1}$), the CN stretching bands in compounds **1** ($\nu_{CN}$ = 2095 $cm^{-1}$) and **2** ($\nu_{CN}$ = 2099 $cm^{-1}$) show a clear shift to higher frequencies and a evident shift to lower frequency for compound **3** ($\nu_{CN}$ = 2077 $cm^{-1}$). This result can be explained by a combination of two factors: back-bonding from the C-bonded metal into the CN bond and kinematic coupling upon cyanide-bridge formation[38-40]. The former effect is expected to be enhanced by the withdrawal of charge from the cyanide to the second metal and shifts *ν*(CN) to a lower frequency, while the latter effect is a mechanical constraint on the CN motion and shifts *ν*(CN) to a higher frequency. For compounds **1** and **2**, the raise of $\nu_{CN}$ can be attributed to the stronger effect of the kinematic coupling than the back-bonding effect. For compound **3**, however, it can be considered that the back-bonding effect is outweighed, suggesting that $Mn^{2+}$ is electron-poorer than $Fe^{2+}$ and $Co^{2+}$.

**Table 3. CN Stretching Frequencies of Complexes 1~3 and Their Parent Mononuclear Compound**

| Complexes | $\nu_{CN}$ ($cm^{-1}$) |
|---|---|
| **$[Fe^{II}(PY_5OMe_2)CN](OTf)$** | 2087 |
| **1** | 2095 |
| **2** | 2099 |
| **3** | 2077 |

### 3. 3 Magnetic properties

The temperature dependence of magnetic susceptibilities for complexes **1**, **2** and **3** was collected in an applied field of 1000 Oe under the temperature range of 2~400 K (Fig. 2). Complexes **2** and **3** were recorded in a cooling mode from 400 to 2 K, and complex **1** was recorded in both cooling and heating modes from 400 to 2 to 400 K. The TGA results of complexes **1**~**3** show that compounds **1** and **2** have lost all solvents at 400 K and these three compounds remain thermally stable in the temperature range of 300~400 K (Fig. S3). The thermal variation of the product of the molar magnetic susceptibility times the temperature ($\chi_M$T) for the Fe(II) complex **1** shows the presence of SCO, as shown in Fig. 2. The value of $\chi_M$T at 400 K is 2.38 $cm^3{\cdot}K{\cdot}mol^{-1}$ slightly below the expected value (3.0 $cm^3{\cdot}K{\cdot}mol^{-1}$) of one HS Fe(II) ion ($S$ = 2, $g$ = 2.0), which means the existence of a small amount of LS Fe(II). On further cooling, there is an obvious decrease in the $\chi_M$T values from 2.38 to 0 $cm^3{\cdot}K{\cdot}mol^{-1}$ from 400 to 300 K, indicating the completion of spin transition from HS to the LS state. In heating processes, the transition occurs from 400 to 336 K, resulting in a hysteresis loop of 36 K. For the Co(II) complex **2**, the $\chi_M$T value is 2.87 $cm^3{\cdot}K{\cdot}mol^{-1}$ at 400 K which is consistent with an octahedral HS Co(II) center with $S$ = 3/2, then the $\chi_M$T product shows a smooth decline and reached 1.74 $cm^3{\cdot}K{\cdot}mol^{-1}$ at 2 K. This magnetic behavior is typical in Co(II) octahedral complex and attributed to the magnetic anisotropy caused by spin-orbit coupling[33-36]. The $\chi_M$T product for the Mn(II) complex **3** basically maintains at around 4.65 $cm^3{\cdot}K{\cdot}mol^{-1}$ in the temperature range of 2~400 K, which is in agreement with the theoretical spin-only values (4.375 $cm^3{\cdot}K{\cdot}mol^{-1}$) for a HS Mn(II) ion ($S$ = 5/2, $g$ = 2.0).

Apparently, these three adjacent transition metal ions

show different magnetic behaviors, although they are in the same ligand field. The Co(II) ion for **2** and Mn(II) ion for **3** are both in a high-spin state through 2~400 K, but the cyanide-nitrogen coordinated Fe(II) ion for complex **1** possesses a SCO behavior over 300 K. Such differences are related to the *d*-orbital splitting of these metal ions, indicating that Fe(II) gives a lager orbital splitting in this ligand field[41].

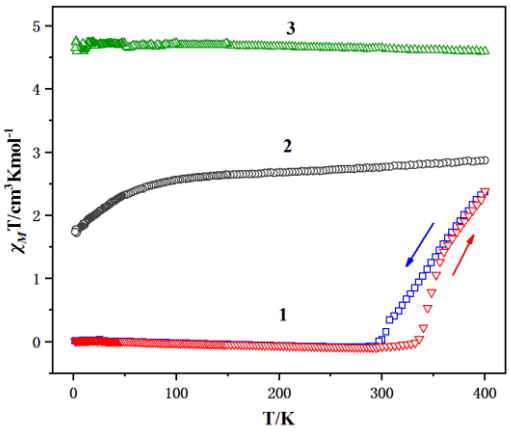


**Fig. 2. Thermal variation of the $\chi_M$T product for complexes 1 (The dashed red and blue lines represent the heating and cooling modes, respectively), 2 (gray) and 3 (green)**

## 4 CONCLUSION

In summary, three dinuclear cyanide-bridged complexes have been designed and synthesized by using the same building unit $[Fe^{II}(PY_5OMe_2)CN]^+$ and mononuclear units $[M^{II}(PY_5OMe_2)]^{2+}$ (M = Fe, Co and Mn) with different metal ions. Single-crystal X-ray diffraction analyses show that the structures of these three dinuclear complexes are very similar. The measured $\nu$(CN) results for compounds **1**~**3** suggest that $Mn^{2+}$ is electron-poorer than $Fe^{2+}$ and $Co^{2+}$. And, the temperature dependence of magnetic susceptibilities suggest that these three compounds have different magnetic behavior, namely compound **1** exhibits a SCO behavior and a hysteresis of 36 K, while **2** and **3** are paramagnetic with the high-spin cyanide-nitrogen bound Co(II) and Mn(II).

## REFERENCES

(1) Shatruk, M.; Avendano, C.; Dunbar, K. R. Cyanide-bridged complexes of transition metals: a molecular magnetism perspective. *Prog. Inorg. Chem.* **2009**, 56, 155−334.

(2) Wang, J. H.; Li, Z. Y.; Yamashita, M.; Bu, X. H. Recent progress on cyano-bridged transition-metal-based single-molecule magnets and single-chain magnets. *Coord. Chem. Rev.* **2021**, 428, 213617−213637.

(3) Wang, J. H.; Vignesh, K. R.; Zhao, J.; Li, Z. Y.; Dunbar, K. R. Charge transfer and slow magnetic relaxation in a series of cyano-bridged $Fe^{III}_4M^{II}_2$ (M = $Fe^{II}$, $Co^{II}$, $Ni^{II}$) molecules. *Inorg. Chem. Front.* **2019**, 6, 493−497.

(4) Su, S. D.; Zhu, X. Q.; Wen, Y. H.; Zhang, L. T.; Yang, Y. Y.; Lin, C. S.; Wu, X. T.; Sheng, T. L. A diruthenium-based mixed spin complex $Ru_2^{5+}$ ($S$ = 1/2)-CN-$Ru_2^{5+}$ ($S$ = 3/2). *Angew. Chem. Int. Ed.* **2019**, 131, 15344−15348.

(5) Yang, Y. Y.; Zhu, X. Q.; Hu, S. M.; Su, S. D.; Zhang, L. T.; Wen, Y. H.; Wu, X. T.; Sheng, T. L. Different degrees of electron delocalization in mixed valence Ru-Ru-Ru compounds by cyanido-/isocyanido-bridge isomerism. *Angew. Chem. Int. Ed.* **2018**, 57, 14046−14050.

(6) Lescouezec, R.; Vaissermann, J.; Ruiz-Perez, C.; Lloret, F.; Carrasco, R.; Julve, M.; Verdaguer, M.; Dromzee, Y.; Gatteschi, D.; Wernsdorfer, W. Cyanide-bridged iron(III)-cobalt(II) double zigzag ferromagnetic chains: two new molecular magnetic nanowires. *Angew. Chem. Int. Ed.* **2003**, 42, 1483−1486.

(7) Wang, S.; Zuo, J. L.; Gao, S.; Song, Y.; Zhou, H. C.; Zhang, Y. Z.; You, X. Z. The observation of superparamagnetic behavior in molecular nanowires. *J. Am. Chem. Soc.* **2004**, 126, 8900−8901.

(8) Toma, L. M.; Lescouezec, R.; Pasan, J.; Ruiz-Perez, C.; Vaissermann, J.; Cano, J.; Carrasco, R.; Wernsdorfer, W.; Lloret, F.; Julve, M. $[Fe(bpym)(CN)_4]^-$: a new building block for designing single-chain magnets. *J. Am. Chem. Soc.* **2006**, 128, 4842−4853.

(9) Hoshino, N.; Iijima, F.; Newton, G. N.; Yoshida, N.; Shiga, T.; Nojiri, H.; Nakao, A.; Kumai, R.; Murakami, Y.; Oshio, H. Three-way switching in a cyanide-bridged [CoFe] chain. *Nat. Chem.* **2012**, 4, 921−926.

(10) Pichon, C.; Suaud, N.; Duhayon, C.; Guihery, N.; Sutter, J. P. Cyano-bridged Fe(II)-Cr(III) single-chain magnet based on pentagonal bipyramid units: on the added value of aligned axial anisotropy. *J. Am. Chem. Soc.* **2018**, 140, 7698−7704.

(11) Sokol, J. J.; Hee, A. G.; Long, J. R. A cyano-bridged single-molecule magnet: slow magnetic relaxation in a trigonal prismatic $MnMo_6(CN)_{18}$ cluster. *J. Am. Chem. Soc.* **2002**, 124, 7656−7657.

(12) Choi, H. J.; Sokol, J. J.; Long, J. R. Raising the spin-reversal barrier in cyano-bridged single-molecule magnets: linear $Mn(III)_2M(III)(CN)_6$ (M = Cr, Fe) species incorporating $[(5\text{-brsalen})Mn]^+$ units. *Inorg. Chem.* **2004**, 43, 1606−1608.

(13) Zhang, Y. Z.; Mallik, U. P.; Clerac, R.; Rath, N. P.; Holmes, S. M. Irreversible solvent-driven conversion in cyanometalate $\{Fe_2Ni\}_n$ (n = 2, 3) single-molecule magnets. *Chem. Commun.* **2011**, 47, 7194−7196.

(14) Cho, K. J.; Ryu, D. W.; Kwak, H. Y.; Lee, J. W.; Lee, W. R.; Lim, K. S.; Koh, E. K.; Kwon, Y. W.; Hong, C. S. Designed cyanide- and phenoxide-bridged Fe(III)Mn(III) single-molecule magnet constructed by highly blocked paramagnetic precursors. *Chem. Commun.* **2012**, 48, 7404−7406.

(15) Saber, M. R.; Dunbar, K. R. Trigonal bipyramidal 5*d*-4*f* molecules with SMM behavior. *Chem. Commun.* **2014**, 50, 2177−2179.

(16) Xin, Y.; Wang, J.; Zychowicz, M.; Zakrzewski, J. J.; Nakabayashi, K.; Sieklucka, B.; Chorazy, S.; Ohkoshi, S. I. Dehydration-hydration switching of single-molecule magnet behavior and visible photoluminescence in a cyanido-bridged Dy(III)Co(III) framework. *J. Am. Chem. Soc.* **2019**, 141, 18211−18220.

(17) Papanikolaou, D.; Margadonna, S.; Kosaka, W.; Ohkoshi, S.; Brunelli, M.; Prassides, K. X-ray illumination induced Fe(II) spin crossover in the Prussian blue analogue cesium iron hexacyanochromate. *J. Am. Chem. Soc.* **2006**, 128, 8358−8363.

(18) Kosaka, W.; Nomura, K.; Hashimoto, K.; Ohkoshi, S. Observation of an Fe(II) spin-crossover in a cesium iron hexacyanochromate. *J. Am. Chem. Soc.* **2005**, 127, 8590−8591.

(19) Jeon, I. R.; Calancea, S.; Panja, A.; Piñero Cruz, D. M.; Koumousi, E. S.; Dechambenoit, P.; Coulon, C.; Wattiaux, A.; Rosa, P.; Mathonière, C.; Clérac, R. Spin crossover or intra-molecular electron transfer in a cyanido-bridged Fe/Co dinuclear dumbbell: a matter of state. *Chem. Sci.* **2013**, 4, 2463−2470.

(20) Li, Z. Y.; Dai, J. W.; Damjanović, M.; Shiga, T.; Wang, J. H.; Zhao, J.; Oshio, H.; Yamashita, M.; Bu, X. H. Structure switching and modulation of magnetic properties in diarylethene-bridged metallosupramolecular compounds via controlled coordination-driven self-assembly. *Angew. Chem. Int. Ed.* **2019**, 58, 4339−4344.

(21) Herchel, R.; Boca, R.; Gembicky, M.; Kozisek, J.; Renz, F. Spin crossover in a tetranuclear Cr(III)-$Fe(III)_3$ complex. *Inorg. Chem.* **2004**, 43, 4103−4105.

(22) Kawabata, S.; Chorazy, S.; Zakrzewski, J. J.; Imoto, K.; Fujimoto, T.; Nakabayashi, K.; Stanek, J.; Sieklucka, B.; Ohkoshi, S. I. *In situ* ligand transformation for two-step spin crossover in $Fe(II)[M(IV)(CN)_8]^{4-}$ (M = Mo, Nb) cyanido-bridged frameworks. *Inorg. Chem.* **2019**, 58, 6052−6063.

(23) Papanikolaou, D.; Kosaka, W.; Margadonna, S.; Kagi, H.; Ohkoshi, S. I.; Prassides, K. Piezomagnetic behavior of the spin crossover Prussian blue analogue $CsFe[Cr(CN)_6]$. *J. Phys. Chem. C* **2007**, 111, 8086−8091.

(24) Kuppusamy, S. K.; Mario, R. Emerging trends in spin crossover (SCO) based functional materials and devices. *Coord. Chem. Rev.* **2017**, 346, 176−205.

(25) Holovchenko, A.; Dugay, J.; Gimenez-Marques, M.; Torres-Cavanillas, R.; Coronado, E.; van der Zant, H. S. J. Near room-temperature memory devices based on hybrid spin-crossover $SiO_2$ nanoparticles coupled to single-layer graphene nanoelectrodes. *Adv. Mater.* **2016**, 28, 7228−7233.

(26) Cowan, M. G.; Olguin, J.; Narayanaswamy, S.; Tallon, J. L.; Brooker, S. Reversible switching of a cobalt complex by thermal, pressure, and electrochemical stimuli: abrupt, complete, hysteretic spin crossover. *J. Am. Chem. Soc.* **2012**, 134, 2892–2894.

(27) Thies, S.; Sell, H.; Schuett, C.; Bornholdt, C.; Naether, C.; Tuczek, F.; Herges, R. Light-induced spin change by photodissociable external ligands: a new principle for magnetic switching of molecules. *J. Am. Chem. Soc.* **2011**, 133, 16243–16250.

(28) Goldsmith, C. R.; Cole, A. P.; Stack, T. D. C–H activation by a mononuclear manganese(III) hydroxide complex: synthesis and characterization of a manganese-lipoxygenase mimic? *J. Am. Chem. Soc.* **2005**, 127, 9904–9912.

(29) Rudd, D. J.; Goldsmith, C. R.; Cole, A. P.; Stack, T. D.; Hodgson, K. O.; Hedman, B. X-ray absorption spectroscopic investigation of the spin-transition character in a series of single-site perturbed iron(II) complexes. *Inorg. Chem.* **2005**, 44, 1221–1229.

(30) Bain, G. A.; Berry, J. F. Diamagnetic corrections and Pascal's constants. *J. Chem. Edu*. **2008**, 85, 532–536.

(31) Sheldrick, G. M. Crystal structure refinement with SHELXL. *Acta. Crystallogr. C Struct. Chem.* **2015**, 71, 3–8.

(32) Phan, H.; Hrudka, J. J.; Igimbayeva, D.; Lawson Daku, L. M.; Shatruk, M. A simple approach for predicting the spin state of homoleptic Fe(II) tris-diimine complexes. *J. Am. Chem. Soc*. **2017**, 139, 6437−6447.

(33) Banci, L.; Bencini, A.; Benelli, C.; Gatteschi, D.; Zanchini, C. Spectral-structural correlations in high-spin cobalt(II) complexes. *Struct. Bond*. **1982**, 52, 37−86.

(34) Benmansour, S.; Setifi, F.; Gómez-García, C. J.; Triki, S.; Coronado, E.; Salaün, J. Y. A novel polynitrile ligand with different coordination modes: synthesis, structure and magnetic properties of the series $[M(tcnoprOH)_2(H_2O)_2]$ (M = Mn, Co and Cu) ($tcnoprOH^-$ = $[(NC)_2CC(OCH_2CH_2CH_2OH)C(CN)_2]^-$). *J. Mol. Struct.* **2008**, 890, 255−262.

(35) Herrera, J. M.; Bleuzen, A.; Dromzee, Y.; Julve, M.; Lloret, F.; Verdaguer, M. Crystal structures and magnetic properties of two octacyanotungstate(IV) and (V)-cobalt(II) three-dimensional bimetallic frameworks. *Inorg. Chem.* **2003**, 42, 7052−7059.

(36) Lloret, F.; Julve, M.; Cano, J.; Ruiz-García, R.; Pardo, E. Magnetic properties of six-coordinated high-spin cobalt(II) complexes: theoretical background and its application. *Inorganica. Chimica. Acta* **2008**, 361, 3432−3445.

(37) Berlinguette, C. P.; Dragulescu-Andrasi, A.; Sieber, A.; Gudel, H. U.; Achim, C.; Dunbar, K. R. A charge-transfer-induced spin transition in the discrete cyanide-bridged complex $[[Co(tmphen)_2]_3[Fe(CN)_6]_2]$. *J. Am. Chem. Soc.* **2005**, 127, 6766−6779.

(38) Alvarez, S.; Lpez, C.; Bermejo, M. J. C−N stretching force constants in cyano complexes: general trends for polycyano, mixed-ligand and cyano-bridged complexes transition. *Met. Chem.* **1984**, 9, 123–126.

(39) Bignozzi, C. A.; Argazzi, R.; Schoonover, J. R.; Gordon, K. C.; Dyer, R. B.; Scandola, F. Electronic coupling in cyano-bridged ruthenium polypyridine complexes and role of electronic effects on cyanide stretching frequencies. *Inorg. Chem.* **1992**, 31, 5260–5267.

(40) Dows, D. A.; Haim, A.; Wilmarth, W. K. Infra-red spectroscopic detection of bridging cyanide groups. *J. Inorg. Nucl. Chem.* **1961**, 21, 33–37.

(41) Halcrow, M. The effect of ligand design on metal ion spin state-lessons from spin crossover complexes. *Crystals* **2016**, 6, 58–78.